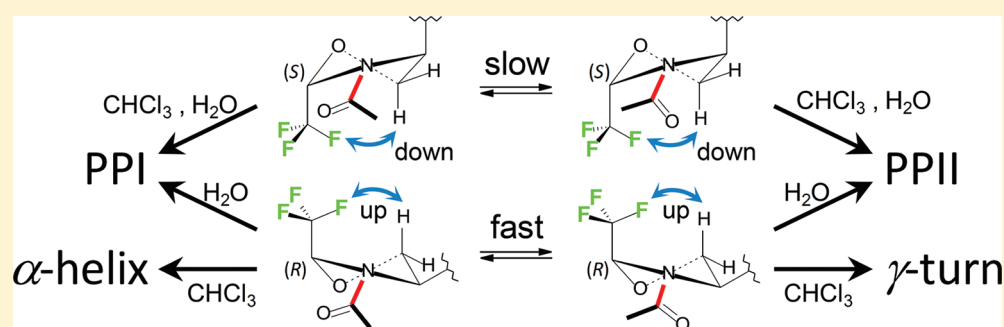


Local Control of the *Cis*–*Trans* Isomerization and Backbone Dihedral Angles in Peptides Using Trifluoromethylated PseudoprolinesDebby Feytens,^{†,‡,§} Grégory Chaume,[¶] Gérard Chassaing,^{†,‡,§} Solange Lavielle,^{†,‡,§} Thierry Brigaud,[¶] Byung Jin Byun,[⊥] Young Kee Kang,^{*,⊥} and Emeric Miclet^{*,†,‡,§}[†]Laboratoire des BioMolécules, UPMC Paris 06, 4, Place Jussieu, 75005 Paris, France[‡]Laboratoire des BioMolécules, Département de Chimie, Ecole Normale Supérieure, 24, rue Lhomond, 75005 Paris, France[§]UMR 7203, FR 2569, 4, Place Jussieu, 75005 Paris, France[¶]Laboratoire SOSCO, Université de Cergy-Pontoise, EA 4505, 5 mail Gay Lussac, 95000 Cergy-Pontoise, France[⊥]Department of Chemistry, Chungbuk National University, Cheongju, Chungbuk 361-763, Republic of Korea

S Supporting Information



ABSTRACT: NMR studies and theoretical calculations have been performed on model peptides Ac-Ser(Ψ Pro)-NHMe, (S,S)Ac-Ser($\Psi^{\text{H,CF}_3}$ Pro)-NHMe, and (R,S)Ac-Ser($\Psi^{\text{CF}_3,\text{H}}$ Pro)-NHMe. Their thermodynamic and kinetic features have been analyzed in chloroform, DMSO, and water, allowing a precise description of their conformational properties. We found that trifluoromethyl C^δ -substitutions of oxazolidine-based pseudoprolines can strongly influence the *cis*–*trans* rotational barriers with only moderate effects on the *cis*/*trans* population ratio. In CHCl_3 , the configuration of the CF_3 – C^δ entirely controls the ψ -dihedral angle, allowing the stabilization of γ -turn-like or PPI/PPII-like backbone conformations. Moreover, in water and DMSO, this C^δ -configuration can be used to efficiently constrain the ring puckering without affecting the *cis*/*trans* population ratio. Theoretical calculations have ascertained the electronic and geometric properties induced by the trifluoromethyl substituent and provided a rational understanding of the NMR observations.

INTRODUCTION

The cyclic nature of the proline residue gives rise to some unique conformational properties of the peptide backbone. First, it induces a constraint by restricting the ϕ dihedral angle to values around -60° .¹ Second, the Xaa–Pro peptide bond is subject to *cis*–*trans* isomerization characterized by an increased *cis* population (lower free energy difference ΔG_{tc}) and an activation energy ($\Delta G^\ddagger_{\text{tc}}$) that is low when compared to the other amino acids (Figure 1).^{2–4} Besides, the five-membered

ring of the Pro residue can adopt two distinct conformations (up-puckered or C^γ -*exo* and down-puckered or C^γ -*endo*)¹ that are almost equally abundant in peptides^{5–7} and proteins.^{2,8,9} A variety of mimics and analogues have been designed in order to control the conformation of the peptide backbone and/or to alter the *cis*/*trans* ratios and the rotational barriers for *cis*–*trans* isomerization.¹⁰ In this context, C^δ -substituted prolines **1** and pseudoprolines (Ψ Pro) **2** have been shown to be very useful, as ΔG_{tc} and $\Delta G^\ddagger_{\text{tc}}$ can be monitored depending on the nature of R_1 and R_2 as well as on the absolute configuration at C^δ .^{11–15} These molecules can be used to tailor *cis*/*trans* isomerization around the Xaa– Ψ Pro amide bond, offering a wide range of applications in peptide engineering.

Theoretical calculations on Pro- and Ψ Pro-containing model peptides, such as Ac-Pro-NHMe, Ac-Oxa-NHMe (Ψ Pro

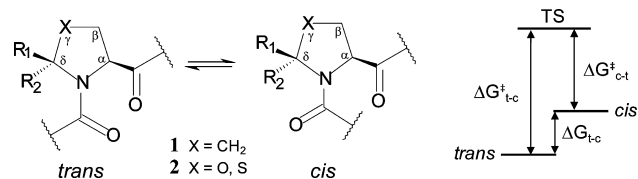


Figure 1. C^δ -substituted prolines **1** and pseudoprolines **2**.

Received: January 10, 2012

Revised: March 1, 2012

Published: March 8, 2012

derived from Ser), and Ac-Thz-NHMe (Ψ Pro derived from Cys) have been reported in which ΔG_{tc}^- and ΔG_{tc}^+ as well as puckering transitions were calculated.^{15–22} When NMR data were available, theoretical calculations showed fair agreement with the observations gathered in solution: (i) replacement of Pro by Ψ Pro resulted in increased *cis* populations and decreased rotational barriers for *cis*–*trans* isomerization, (ii) presence of R_1 substituents further decreased the rotational barriers, and (iii) presence of R_2 substituents caused major increases of the *cis* populations.

In the course of our investigations on the stereoselective synthesis of trifluoromethyl group containing amino acids (Tfm-AAs) and their incorporation into peptides,²³ we have recently reported the synthesis of CF_3 -substituted pseudoproline (CF_3 - Ψ Pro) as hydrolytically stable proline surrogates.²⁴ Compared with other prolines or pseudoproline substituents described in the literature, CF_3 is unique being a bulky group,²⁵ which displays strong inductive effects.²⁶ Moreover, by analogy with Tfm-AAs and pseudopeptides,²⁷ specific effects are expected from the incorporation of CF_3 - Ψ Pro into peptides such as a better stability toward proteases, an increase in lipophilicity, and a better affinity for lipid membranes.²⁸ Herein, we establish the pronounced stereoelectronic influence of the trifluoromethyl C^δ -substituent, in both possible configurations, of the Ser-derived pseudoproline, i.e., (4*S*)-oxazolidine-4-carboxylic acid (Oxa), on the thermodynamic and geometrical properties of model peptides. Both parameters were studied by NMR and theoretical calculations on the pseudopeptides: Ac-Ser(Ψ Pro)-NHMe (Oxa peptide) (3), (2*S*,4*S*)Ac-Ser(Ψ^{H,CF_3} Pro)-NHMe (2(*S*)- CF_3 -Oxa peptide) (4), and (2*R*,4*S*)Ac-Ser($\Psi^{CF_3,H}$ Pro)-NHMe (2(*R*)- CF_3 -Oxa peptide) (5), shown in Figure 2.

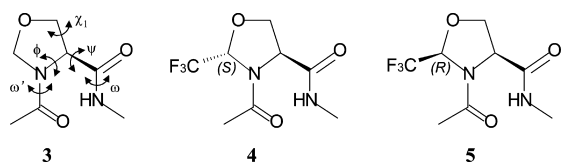


Figure 2. Model peptides 3, 4 and 5 used in this study.

MATERIALS AND METHODS

Conformational Analysis by NMR. NMR experiments were recorded on a Bruker Avance III spectrometer operating at a 1H frequency of 500 MHz and equipped with a triple resonance, z -axis pulsed-field-gradient cryogenic probe head, optimized for 1H detection. Data were processed using TOPSPIN software using shifted sine-bell window functions and extensive zero-filling prior to Fourier transformation to yield high digital resolution. NMR samples were prepared by dissolving 2.5 mg of each compound in 600 μL of solvent (DMSO- d_6 ; 0.03% TMS in $CDCl_3$; 1% (v/v) DSS in $D_2O:H_2O$ 1:9). Residual DMSO, TMS, or DSS signals were used to calibrate the chemical shift. 2D COSY and TOCSY experiments (mixing time of 80 ms, typically collected as 1024 (t1) and 2048 (t2) time-domain matrices over a spectral width of 10 ppm, with 16 scans per t1 increment) were recorded to obtain the complete proton assignments. Carbon assignments were obtained from heteronuclear 2D 1H – ^{13}C HSQC spectra using 512 (t1) and 1024 (t2) time-domain matrices over a spectral width of 10 ppm, with 32 scans per t1 increment or from CH_2 -

TROSY experiments.²⁹ 2D ROESY and NOESY experiments reflecting the spatial proximity between the CH_3 acetyl group and the H^α or H^δ protons were used to assign the *trans* and *cis* conformations, respectively (mixing time from 300 ms to 1 s, typically collected as 1024 (t1) and 2048 (t2) time-domain matrices over a spectral width of 10 ppm, with 16 scans per t1 increment). $^3J_{H\alpha-H\beta/2}$ and $^3J_{H\alpha-H\beta/3}$ coupling constants used to determine the ring puckering were obtained from well-resolved 1D spectra or from CH_2 -TROSY experiments.³⁰ *Cis*–*trans* isomerization rate constants were determined from the coalescence temperatures observed in 1D spectra (temperature studies between 233–323 K in $CDCl_3$, 277–362 K in $D_2O:H_2O$ 1:9, or 292–362 K in DMSO- d_6).^{31,32} For each sample, typically three coalescence temperatures were determined on three couples of resonances, which were used for the calculation of independent rate constants. An additional method was tested for the measurements of rate constants, which is based on 2D EXSY experiments employing short mixing times (from 20 to 100 ms).¹⁴ A very good agreement with the coalescence temperature method was obtained. Rotational barriers were then calculated using the Eyring equation.

Computational Methods. Chemical structures and torsional angles for the peptides 3, 4, and 5 are defined in Figure 2. All ab initio HF and hybrid density functional B3LYP calculations were carried out using the Gaussian 03 package.³³ The 10 local minima (*tAd*, *tCd*, *tFd*, *tAu*, *tCu*, *tFu*, *cAd*, *cFd*, *cAu*, and *cFu*) and four transition states (*ts1*–*ts4*) for the Oxa peptide 3 optimized at the HF/6-31+G(d) level of theory in the gas phase and in solution (chloroform and water)²¹ were used to generate the initial structures for both the CF_3 -Oxa peptides 4 and 5 using the GaussView program.³⁴ Then, all these initial structures were optimized at the same HF/6-31+G(d) level of theory in the gas phase and in solution. The first letter of each conformational letter code depicts the geometry of the ω' prolyl peptide bond, either *cis* (*c*) or *trans* (*t*). The second informs about the (ϕ , ψ) backbone dihedral angles that correspond to the α -helical (*A*), γ -turn (*C*), or polyproline-like (*F*) regions of the Ramachandran diagram. The last letter depends on the χ_1 angle of the oxazolidine ring and accounts for the up (*u*) or down (*d*) puckering.

We employed the conductor-like polarizable continuum model (CPCM),³⁵ implemented in the Gaussian 03 package,³³ to compute solvation free energies (ΔG_s) at the HF/6-31+G(d) level of theory with the UAKS cavities, which are the united atom topological model (UATM) radii optimized at the density functional PBE0/6-31G(d) level of theory.³⁶ The solvation free energy is the sum of the electrostatic free energy and the nonelectrostatic energy terms. The latter is composed of the cavitation, dispersion, and repulsion energy terms. For CPCM-UAKS calculations, the default average areas of 0.2 \AA^2 for tesseræ were used. The dielectric constants of chloroform and water used here are 4.9 and 78.4 at 25 $^\circ C$, respectively.

The structures of the transition states *ts1* and *ts2* are similar to the *syn/exo* structures with down and up puckerings, respectively, whereas those of *ts3* and *ts4* resemble the *anti/exo* structures with down and up puckerings, respectively, according to the definition of Fischer et al. in ref 37. Each transition state was checked by the intrinsic reaction coordinate (IRC) method³⁸ whether it connects the reactants and products, that is, the *trans* and *cis* conformers. However, as in most cases, the IRC calculation did not step all the way to the minimum on either side of the path.³⁹ Further optimizations were carried out

Table 1. Thermodynamic Properties of 3, 4, and 5 As Determined by NMR Spectroscopy^a

solvent		3	4	5
CDCl ₃	<i>cis:trans</i>	(27 ± 3):(73 ± 3)	(40 ± 2):(60 ± 2)	(24 ± 3):(76 ± 3)
	ΔG°_{tc} ^b	0.59	0.24	0.68
	ΔG^{\ddagger}_{tc}	16.74 ± 0.27	16.71 ± 0.26	14.77 ± 0.25
	ΔG^{\ddagger}_{ct}	16.10 ± 0.27	16.43 ± 0.26	14.07 ± 0.25
DMSO- <i>d</i> ₆	<i>cis:trans</i>	(46 ± 2):(54 ± 2)	(66 ± 2):(34 ± 2)	(55 ± 2):(45 ± 2)
	ΔG°_{tc} ^b	0.09	−0.39	−0.12
	ΔG^{\ddagger}_{tc}	17.77 ± 0.25	16.77 ± 0.25	15.32 ± 0.25
	ΔG^{\ddagger}_{ct}	17.66 ± 0.25	17.22 ± 0.25	15.46 ± 0.25
D ₂ O:H ₂ O 1:9	<i>cis:trans</i>	(34 ± 2):(66 ± 2)	(43 ± 2):(57 ± 2)	(45 ± 2):(55 ± 2)
	ΔG°_{tc} ^b	0.39	0.17	0.12
	ΔG^{\ddagger}_{tc}	18.41 ± 0.23	18.06 ± 0.27	15.63 ± 0.23
	ΔG^{\ddagger}_{ct}	17.93 ± 0.23	17.88 ± 0.27	15.51 ± 0.23

^aAll energies are given in kcal/mol. ^bFrom $\Delta G^{\circ}_{tc} = -RT \ln K_{tc}$, where $K_{tc} = [cis]/[trans]$ at $T = 298.15$ K.

starting from the reactants and products obtained by the IRC method to reach the two minima that the transition state connects.

Vibrational frequencies were calculated for all stationary points at the HF/6-31+G(d) and CPCM HF/6-31+G(d) levels of theory in the gas phase and in solution, respectively, which were used to compute enthalpies and Gibbs free energies at 25 °C and 1 atm. The scale factor of 0.89 was chosen to reproduce experimental frequencies for the amide I band of *N*-methylacetamide in Ar and N₂ matrixes.⁴⁰ In particular, each transition state was confirmed by checking whether it has one imaginary frequency after frequency calculations. The zero-point energy correction and the thermal energy corrections were used to calculate the enthalpy (*H*) and entropy (*S*) of each conformation.^{41,42} Here, the ideal gas, rigid rotor, and harmonic oscillator approximations were used for the translational, rotational, and vibrational contributions to the Gibbs free energy, respectively. The B3LYP/6-311++G(d,p) single-point energies were calculated for all local minima and transition states of two peptides 4 and 5 located at the HF/6-31+G(d) level of theory in the gas phase and the CPCM HF/6-31+G(d) level of theory in solution. The B3LYP/6-311++G(d,p)//CPCM HF/6-31+G(d) level of theory provided the populations of backbone and prolyl peptide bond for the proline¹⁷ and pseudoproline²¹ peptides that are comparable with the observed values in chloroform and water.

The bond overlap index and the atomic charges of the carbonyl C and the prolyl nitrogen of the C–N bond for the privileged *trans* and transition-state conformers of each of three peptides 3–5 in chloroform and water were calculated at the B3LYP/6-311++G(d,p) level of theory using the natural bond orbital (NBO) method⁴³ implemented in the Gaussian 03 package.³³ The Wiberg bond index⁴⁴ obtained by the sums of squares of off-diagonal density matrix elements of the C–N bond can be used as a measure of a bond overlap. In addition, second-order perturbation energies calculated at the B3LYP/6-311++G(d,p) level of theory, which reflect the strength of donor → acceptor (or bonding → antibonding) hyperconjugative interactions between NBOs,^{43b} were used to analyze the relative stabilities of the down and up puckerings and the transition states for peptides 4 and 5.

RESULTS

The CF₃-Oxa-containing peptides 4 and 5 chosen for this study are displayed in Figure 2. The unsubstituted Oxa peptide 3 was included in order to distinguish the effects related to the ring

oxygen versus those resulting from the CF₃ group (for synthesis details, see section S1 of the Supporting Information). Theoretical studies on 3 were previously reported, but to our knowledge no experimental data are available.^{17,21,22}

NMR Analysis of the *Cis*–*Trans* Isomerization. The *cis*–*trans* equilibrium was studied by ¹H NMR in CDCl₃, DMSO-*d*₆, and D₂O:H₂O 1:9 solutions by recording spectra at different temperatures. In all solvents, two sets of ¹H resonances were observed at the lowest temperatures for 3–5, clearly indicating the presence of two slowly exchanging conformations (Figures S1–S3 of the Supporting Information). 2D NMR experiments allowed us to unambiguously assign the *cis* ($\omega' = 0^\circ$) and the *trans* ($\omega' = 180^\circ$) conformers, the CH₃ acetyl group being in close proximity to the H^α or H^β, respectively. The *cis*/*trans* populations were determined by simple integration of the resonances and were found independent of the temperature in the range tested. *Cis*/*trans* ratios are reported in Table 1, together with the corresponding Gibbs energy ΔG° .

In chloroform, introducing the (2*R*)-CF₃ substituent at the C^δ-position of the Oxa ring (5) has virtually no influence on the *cis* population in contrast to the (2*S*)-CF₃ substituent (4), which significantly stabilizes the *cis* content. In water and DMSO, increased *cis* contents are observed for all the three peptides when compared to chloroform, with median values of 43% and 55%, respectively. Peptide 3 incorporating the unsubstituted Oxa typically displays ~10% lower *cis* content than 4 and 5 in these polar solvents. However, relatively high *cis* content is observed for 4 in DMSO (66%).

The coalescence temperature method was used to determine the rotational barriers for *cis*–*trans* isomerization.³¹ The results are shown in Table 1. For a given molecule, ΔG^{\ddagger}_{tc} and ΔG^{\ddagger}_{ct} increase with the polarity of the solvent, as already reported for Ac-Pro-NHMe,¹⁹ and as expected, since polar solvents normally stabilize both ground states (partially charged) and destabilize the transition state. When compared to the unsubstituted ring in peptide 3, a CF₃-substituent with the (2*S*) configuration does not alter ΔG^{\ddagger}_{ct} to a great extent, whereas the (2*R*) configuration at C^δ-position significantly decreases the rotational barrier by about 2 kcal/mol.

H-Bond Study. In order to examine the presence of an intramolecular H-bond between the C-terminal amide NH and the carbonyl of the *N*-terminal acetyl group, the solvent dependences of the NH chemical shift were studied.⁴⁵ The results are shown in Table 2. For peptides 3 and 5, the chemical shifts of the NH protons in the *trans* conformation are much less influenced by the solvent than the NH protons in the *cis*

Table 2. Solvent and Temperature Dependence of the NH Chemical Shift

entry	$\Delta\delta_{\text{NH}}$ at 283 K (ppm)		$\Delta\delta_{\text{NH}}/\Delta T$ (ppb/K)	
	$\text{CDCl}_3 \rightarrow \text{DMSO}-d_6$	$\text{CDCl}_3 \rightarrow \text{water}$	$\text{DMSO}-d_6$	water
3 <i>cis</i>	1.92	2.21	−4.0	−7.1
3 <i>trans</i>	0.86	1.19	−3.6	−7.0
4 <i>cis</i>	2.53	2.66	−4.0	−7.3
4 <i>trans</i>	2.01	2.34	−4.2	−7.5
5 <i>cis</i>	1.93	2.14	−5.3	−7.8
5 <i>trans</i>	1.01	1.35	−4.8	−7.9

conformation, as demonstrated by their $\Delta\delta_{\text{NH}}$ values. This is indicative of the presence of an intramolecular H-bond in the *trans* conformations, which is absent in the *cis* conformations. In pseudotripeptide 4, the NH protons show a similar solvent dependence indicating the absence of an H-bond in either conformation. Additionally, the temperature influences on the NH chemical shifts were analyzed in polar solvents (Table 2).⁴⁵ Temperature coefficients in water are of the same magnitude for all peptides in both *cis* and *trans* conformations (ca. −7.5 ppb/K), indicating that no intramolecular H-bonds are present at all. The H-bonds observed in the *trans* conformations of 3 and 5 in chloroform are clearly not strong enough to compete with water. In DMSO, all T -coefficients ($\Delta\delta_{\text{NH}}/\Delta T$) were found lower than −3 ppb/K. This value has been used in DMSO to discriminate between solvent-shielded amide protons engaged in intramolecular H-bond (high T -coefficients) and amide protons of unstructured peptides (low T -coefficients).⁴⁶ However, T -coefficients greater than −3 ppb/K are usually measured on cyclic peptides and this cutoff value appears inadequate for small-sized noncyclic peptides. Hence, we used the difference of the T -coefficients in the two peptide bond conformations as an indicator of the propensity to form H-bonds. Significant increases are observed in 3 (+0.4 ppb/K) and 5 (+0.5 ppb/K) when rotating the prolyl peptide bond from *cis* to *trans* conformation, suggesting that the H-bonds observed in CDCl_3 for the 3 and 5 *trans* conformers are still weakly stabilized in DMSO.

Puckering. The puckering of the five-membered ring in pseudoproline residues can be determined from the coupling constants between the α and β protons. As shown in Figure 3a, the α proton appears as a triplet (t) in the up-puckered form, and as a doublet of doublets (d \times d) in the down-puckered form; H^α – H^β vicinal coupling constants can be determined on the H^α resonances, provided that well-resolved 1D spectra are obtained. More generally, the precise determination of the vicinal couplings are reliably extracted from the H^β resonances in the CH_2 -TROSY experiment since (i) the ^{13}C dimension offers spectral dispersion and (ii) the geminal 2J coupling is removed.³⁰ Such a spectrum is shown in Figure 3b, all extracted vicinal couplings being reported in Table 3. Note that for peptide 5 in CDCl_3 and DMSO, no coupling constant can be precisely determined due to a faster exchange between the *cis* and *trans* conformations, which broadens the peaks.

The results clearly indicate that for peptides 4 and 5 one puckering is found for both the *cis* and *trans* conformations, whatever the solvent. However, this puckering depends on the absolute configuration at C^δ , peptide 4 being observed as a down-puckered form whereas peptide 5 adopts the up-puckered conformation. For the unsubstituted peptide 3, a slightly different result is obtained. In CDCl_3 and DMSO, 3 mainly presents the down-puckered form, but *trans* states are

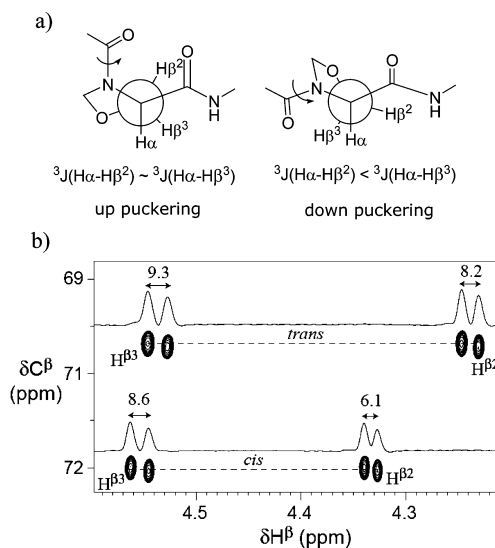


Figure 3. (a) Newmann projections of the two possible ring puckerings, and (b) βCH_2 region of the CH_2 -TROSY spectrum recorded on 5 in D_2O , 293 K. Cross sections consist of two doublets, which enable the measurement of $^3J(H^\alpha H^{\beta 3})$ and $^3J(H^\alpha H^{\beta 2})$. For each conformer, vicinal coupling values have been reported in hertz.

characterized by higher $^3J(H^\alpha H^{\beta 2})$ values (ca. 3.6 Hz). This is probably the consequence of a small population of up-puckered rings in fast exchange with the major down-puckered conformer. In water, such rapid exchange occurs for 3, being even more pronounced for the *cis* conformer.

Theoretical Calculations. Preferred Conformations. The backbone torsion angles, the endocyclic torsion angles, and the thermodynamic properties of local minima and transition states for (2S)- and (2R)- CF_3 -Oxa peptides 4 and 5, calculated at the B3LYP/6-311++G(d,p)//CPCM HF/6-31+G(d) level of theory in chloroform and water, are listed in Tables S1 and S2 of the Supporting Information. All calculated data for the Oxa peptide 3 at the same level of theory were taken from ref 21. In addition, the preferred structures of local minima and transition states for peptides 4 and 5 optimized in chloroform and water are shown in Figures S4 and S5 of the Supporting Information, respectively, and the corresponding structures of peptide 3 in water are shown in Figure 5 of ref 21.

The populations of all local minima for the three peptides in chloroform and water are listed in Table 4. All populations were obtained by electronic energies (ΔE_e) in solution at 25 °C, since the Gibbs free energies of the (2S)- CF_3 peptide 4 in chloroform and the (2R)- CF_3 peptide 5 in water resulted in an overestimation of the *cis* populations (80.1% and 62.8%, respectively, from Tables S1 and S2 of the Supporting Information), compared to the NMR experimental values (40% and 45%, respectively, see Table 1). However, similar values of *cis* populations were obtained for peptide 3 by electronic energies and Gibbs free energies in chloroform and water.

Backbone Populations. Using the distribution of populations reported in Table 4, the populations of the backbone conformations C, A, and F and the *cis* conformers can be calculated. The (2S)- CF_3 substituent led to the major (over 90%) PP-like conformations (F), and the highest percent of *cis* peptide conformer, with ~40% in chloroform and water. The (2R)- CF_3 substituent led to backbone populations and *cis* peptide bond similar to those observed for the unsubstituted

Table 3. Major Ring Puckerings Deduced from the H^{α} Multiplets and Vicinal Coupling Constants (in hertz) Measured on the $H^{\beta 2}$ and $H^{\beta 3}$ Resonances for 3, 4, and 5

solvent		3 <i>cis</i>	3 <i>trans</i>	4 <i>cis</i>	4 <i>trans</i>	5 <i>cis</i>	5 <i>trans</i>
$CDCl_3$	H^{α} multiplet	d × d	d × d	d × d	d × d	t	t
	$^3J(H^{\alpha}-H^{\beta 2})$	2.0	3.5	<2.0	<2.5	—	—
	$^3J(H^{\alpha}-H^{\beta 3})$	7.1	7.0	7.70	7.80	—	—
$DMSO-d_6$	H^{α} multiplet	d × d	d × d	d × d	d × d	t	t
	$^3J(H^{\alpha}-H^{\beta 2})$	3.1	3.7	2.0	<2.5	—	—
	$^3J(H^{\alpha}-H^{\beta 3})$	7.0	7.2	6.8	8.0	—	—
D_2O	H^{α} multiplet	t	d × d	d × d	d × d	t	t
	$^3J(H^{\alpha}-H^{\beta 2})$	3.8	3.6	2.8	<2.3	6.1	8.2
	$^3J(H^{\alpha}-H^{\beta 3})$	5.3	7.2	7.7	8.3	8.6	9.3

Table 4. Populations (%) of All Local Minima of Peptides 3–5 Calculated at the B3LYP/6-311++G(d,p)//CPCM HF/6-31+G(d) Level of Theory in Chloroform and Water^a

solvent	cAd	cAu	cFd	cFu	tAd	tAu	tCd	tCu	tFd	tFu
Oxa 3 ^b										
chloroform	8.9	2.1	1.1	2.0	6.3	2.7	43.5	24.1	2.5	6.7
water	9.4	1.9	9.8	11.5	16.3	2.7	0.5	nc	27.1	20.7
(2S)-CF ₃ -Oxa 4										
chloroform	3.6	0.0	35.8	0.4	4.7	nc	nc	nc	53.5	2.0
water	0.7	0.0	36.8	0.1	1.3	nc	nc	nc	60.3	0.7
(2R)-CF ₃ -Oxa 5										
chloroform	2.2	7.0	0.0	5.2	nc	5.4	25.8	43.8	0.1	10.6
water	0.3	1.5	0.5	38.3	0.7	4.3	nc	nc	1.1	53.4

^aPopulations (%) were calculated using the Boltzmann statistical weights by relative electronic energies at 25 °C, depending on the *trans/cis* prolyl peptide bonds and down/up puckerings for local minima in Tables S1 and S2 of the Supporting Information. ^bEstimated from data in ref 21. nc denotes not converged calculations.

peptide 3 in chloroform and for the (2S)-CF₃ peptide 4 in water.

Puckering Preferences. The puckering preferences of peptides 3–5, listed in Table 5, were calculated using the

Table 5. Populations of Prolyl Peptide Bond with Puckering for Oxa Peptides 3–5 Calculated at the B3LYP/6-311++G(d,p)//CPCM HF/6-31+G(d) Level of Theory in Chloroform and Water^a

solvent	<i>trans</i> /down	<i>trans</i> /up	<i>cis</i> /down	<i>cis</i> /up
Oxa 3 ^b				
chloroform	52.3	33.5	10.0	4.2
water	44.0	23.4	19.2	13.4
(2S)-CF ₃ -Oxa 4				
chloroform	58.2	2.0	39.4	0.4
water	61.6	0.7	37.6	0.1
(2R)-CF ₃ -Oxa 5				
chloroform	25.8	59.7	2.2	12.2
water	1.8	57.7	0.8	39.7

^aPopulations (%) were calculated using the Boltzmann statistical weights by relative electronic energies at 25 °C, depending on the *trans/cis* prolyl peptide bonds and down/up puckerings for local minima in Tables S1 and S2 of the Supporting Information.

^bEstimated from data in ref 21.

distribution of populations reported in Table 4. For the unsubstituted peptide 3, the *trans*/down conformation is preferred, followed by the *trans*/up conformation in both chloroform and water. Comparable down:up ratios of ~60:40 are observed in both solvents. Although the *trans*/down conformations are privileged (~60%) for the (2S)-CF₃ peptide

4, the *cis*/down conformation becomes largely populated (~40%) in both chloroform and water. This indicates the preference for the down puckering for peptide 4 in both solvents. For the (2R)-CF₃ peptide 5, the *trans*/up conformation is predominant (~60%) in both chloroform and water, followed by the *trans*/down conformation in chloroform (26%) and the *cis*/up conformation in water (40%). This indicates the preference for the up puckering for peptide 5 in both chloroform and water.

Prolyl *Cis*–*Trans* Isomerization. We located four transition states ts1–ts4 with the *syn/exo* and *anti/exo* structures for the *cis*–*trans* isomerization of the Ac–Oxa peptide bond for peptide 3 at the CPCM HF/6-31+G(d) level of theory in chloroform and water,²¹ as found for the Pro peptide.¹⁹ For (2S)-CF₃ peptide 4, only ts2 is located in chloroform and ts1 and ts2 in water (see Table S1 of the Supporting Information). The (2R)-CF₃ peptide 5 has four ts1–ts4 in chloroform and three ts1, ts2, and ts4 in water (see Table S2 of the Supporting Information). In both chloroform and water, ts2's of peptides 3 and 4 are found to have the relative lowest electronic energies, whereas ts1 is favored for peptide 5. However, the prolyl *cis*–*trans* isomerizations of all three peptides proceed through the clockwise rotation with $\omega' \approx +120^\circ$, as found for the Pro peptide.¹⁹ The unsubstituted peptide 3 has the comparable electronic energies for ts2 and ts4 in water.²¹ For each peptide 3–5 in chloroform and water, the relative electronic energies, enthalpies, and Gibbs free energies of the favored transition state and the corresponding privileged *trans* conformation with the lowest electronic energy at the B3LYP/6-311++G(d,p)//CPCM HF/6-31+G(d) level of theory were used to calculate the changes in electronic energy (ΔE_{tc}^\ddagger), enthalpy (ΔH_{tc}^\ddagger),

and Gibbs free energy (ΔG_{tc}^\ddagger) for the prolyl *trans*-to-*cis* isomerization. All the results are summarized in Table 6.

Table 6. Calculated Changes in Electronic Energy, Enthalpy, and Gibbs Free Energy for the Prolyl *Trans*-to-*Cis* Isomerization at the B3LYP/6-311++G(d,p)//CPCM HF/6-31+G(d) Level of Theory in Chloroform and Water^a

solvent	ΔE_{tc}^\ddagger	ΔH_{tc}^\ddagger	ΔG_{tc}^\ddagger	$\Delta G_{tc,exptl}^\ddagger$ ^b
		Oxa 3		
chloroform	17.05	16.13	17.03	16.74 ± 0.27
water	17.77	17.04	18.54	18.41 ± 0.23
		(2S)-CF ₃ -Oxa 4		
chloroform	19.76	19.46	18.47	16.71 ± 0.26
water	21.43	20.48	21.66	18.06 ± 0.27
		(2R)-CF ₃ -Oxa 5		
chloroform	14.46	13.83	14.22	14.77 ± 0.25
water	16.88	16.59	16.70	15.63 ± 0.23

^aUnits in kcal/mol. ΔH_{tc}^\ddagger and ΔG_{tc}^\ddagger at 298.15 K. ^bFrom Table 1.

The rotational barriers ΔG_{tc}^\ddagger for unsubstituted peptide 3 were estimated to be 17.03 and 18.54 kcal/mol in chloroform and water, respectively, which are in very good agreement with the values observed by NMR. However, the rotational barriers ΔG_{tc}^\ddagger for the (2S)-CF₃ peptide 4 were computed to be 18.47 and 21.66 kcal/mol in chloroform and water, respectively, which are slightly higher than the values observed by NMR. Finally, the barriers ΔG_{tc}^\ddagger calculated for the (2R)-CF₃ peptide 5 were found to be lower by ~2 kcal/mol compared with those calculated for the unsubstituted peptide 3. It is interesting to quote that the calculated rotational barriers for peptides 3–5, which are consistent with the results obtained from NMR experiments, increase from chloroform to water in parallel to solvent polarity, as found for Pro dipeptide.¹⁹ Analysis of the contributions to the rotational barriers shows that the prolyl *trans*-to-*cis* isomerization for the Oxa and its (2S)- and (2R)-CF₃ derivatives are entirely enthalpy driven in chloroform and water, with a consequent contribution of the electronic energies.¹⁹ The entropic contributions ($-T\Delta S_{tc}^\ddagger$) range from 0.11 to 1.50 kcal/mol in chloroform and water, except for the (2S)-CF₃ peptide 4 in chloroform with -0.99 kcal/mol. This is consistent with the experimental results with proline-containing peptides, kinetically determined as a function of temperature.⁴⁷

DISCUSSION

Comparison of Experimental and Theoretical Results.

In chloroform, calculations carried out on the Oxa peptide 3 showed 10 local minima and its privileged conformation was found to be *tCd* (43.5%) followed by *tCu* (24.1%) and *cAd* (8.9%) conformations.²¹ This was in very good agreement with the NMR data, showing a predominating down puckering for both *trans* and *cis* isomers with a H-bond detected for the *trans* conformer. Indeed, the backbone conformation C that is preferred for peptide 3 in the *trans* conformation (67.7%) corresponds to a C₇ H-bonded γ -turn between the acetyl and $-NHMe$ terminal groups. However, both the ψ torsion angle and the ring of peptide 3 seemed to be highly dynamic in water since the *cFu*, *cFd*, and *cAd* conformations were almost equally populated in the *cis* form (11.5%, 9.8%, and 9.4%, respectively) and the *trans* form distributed also over three conformations (*tFd* 27.1%, *tFu* 20.7%, and *tAd* 16.3%). The flexibility of the oxazolidine ring was also observed by NMR as quoted by the averaged $^3J(H^aH^{\beta 3})$ and $^3J(H^aH^{\beta 2})$ coupling constants.

Although a slight discrepancy (~10%) was observed for the *cis/trans* ratio determined by NMR and calculations in chloroform (27:73 and 14.2:85.8 by NMR and calculations, respectively), a very good agreement was obtained in water (34:66 and 32.6:67.4 by NMR and calculations, respectively), highlighting the accuracy of the quantum mechanical calculations studied here.

Incorporation of the (2S)-CF₃ substituent caused marked effects on the conformational preferences. The privileged conformation for the (2S)-CF₃ peptide 4 was found to be a PPII-like structure *tFd* with a *trans* peptide bond in both chloroform and water, with 53.5% and 60.3% populations, respectively, followed by the PPI-like structure *cFd* with a *cis* peptide bond (35.8% and 36.8% in chloroform and water, respectively). Thus, the backbone conformation F coupled with a down ring puckering was highly preponderant for peptide 4, regardless of the ω' angle or the solvent polarity. Here again, the data obtained by calculations corroborated NMR results, with down puckerings unambiguously observed in all solvents for both the *cis* and *trans* conformations. Whatever the solvent, none of the γ -turn structures *tCd* or *tCu* was found to be feasible with the calculations, consistent with NMR experiments, and suggesting the absence of an H-bond between the acetyl and $-NHMe$ terminal groups. The calculated *cis* populations for peptide 4 were 39.8% in chloroform and 37.7% in water, in good agreement with those determined by NMR (40% and 43%, respectively) (Table 1).

Finally, the (2R)-CF₃ substituent (peptide 5) exhibited different preferences for the peptide backbone and puckering, compared to the (2S)-CF₃ peptide 4. In chloroform, the privileged conformation of peptide 5 was found to be the *tCu* (43.8%), followed by the *tCd* (25.8%) and *tFu* (10.6%) conformations. However, the PPII-like structure *tFu* with a *trans* peptide bond (53.4%) and the PPI-like structure *cFu* with a *cis* peptide bond (38.3%) prevailed in water. This indicates that the (2R)-CF₃ substituent strongly destabilized the down puckering, thus leading to predominant up populations (71.9% and 97.5% in chloroform and water, respectively). In contrast to peptide 4, the lowest energy structure of peptide 5 in chloroform displayed typical ϕ and ψ torsion angles of the γ -turn (conformation C), whereas the PP-like conformation F was preferred in water. This finding is in good agreement with the NMR results since a H-bond was detected for peptide 5 in CDCl₃. The calculated *cis* populations for peptide 5 were found to be 14.5% and 40.5% in chloroform and water, respectively, which were reasonably consistent with the values of 24% and 45%, respectively, determined by NMR experiments, although there are some underestimations.

Structural Characteristics of the *Cis* and *Trans* Conformers. The structural comparison of the two diastereomers 4 and 5 aimed to identify the parameters which account for the *cis*–*trans* equilibrium. Analysis of the chemical shifts of the (2R)-CF₃ peptide 5 revealed that the methylamide proton was involved in a hydrogen bond only in the *trans* conformer. Such a H-bond was also found in the *trans* peptide 3 but not for peptide 4. This result was in line with the higher populations of the *trans* conformers observed in chloroform and in DMSO for peptides 3 and 5 compared to peptide 4. Interestingly, methyl ester analogues of 4 and 5 lacking the methylamide proton shared similar *cis/trans* populations.²⁴ The presence of a hydrogen bond between the acetyl and the terminal methylamide must lead to a seven-membered C₇ ring that should stabilize the *trans* conformations. Not surprisingly, such

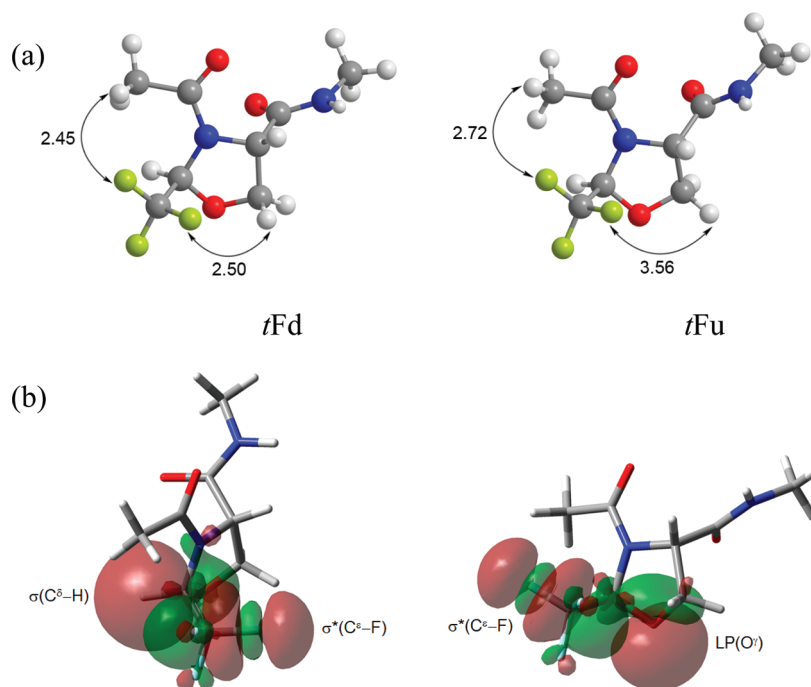


Figure 4. (a) Main F...H electrostatic interactions observed for the minimized *tFd* and *tFu* structures of peptide 4 in water. Distances are denoted in angstroms. (b) The $C^\epsilon-F$ antibonding orbitals are involved in two hyperconjugations that stabilized the down pucker in peptide 4 (*tFd* conformer in water).

γ -turns were disrupted in water due to its high polarity index, yielding very similar *cis/trans* population ratio for peptides 3–5. Previous studies have highlighted the importance of the configuration of the substituted C^δ on the *cis/trans* populations. (*S*)-Alkyl substitutions of prolines,^{11,12,16} oxazolidine,¹⁴ or thiazolidine^{14,15} were always characterized by higher *cis/trans* ratio than with the (*R*)-substituent. Regarding CF_3 substituents, such an imbalance is only observed in $CDCl_3$, where the H-bond stabilized the *trans* conformer of the (2*R*)- CF_3 peptide 5. It has been also reported that increasing the solvent polarity was responsible for the depopulation of the C conformations encompassing this C_7 intramolecular hydrogen bonds.^{19,21} This was accompanied with an increase of the PPII- or PPI-like populations (F conformations). Such behavior occurred for peptide 5, with a dramatic increase in the F population from 15.9% in chloroform to 93.2% in water. However, in all solvents, peptide 5 was highly stabilized with an up puckering, contrasting with the ring of unsubstituted pseudoproline that experienced more dynamics. In particular, the up puckering of peptide 5 was maintained in its *cis* state, whereas proline and non-fluorinated pseudoproline residues preferentially adopted a down puckering.^{9,19,21} Peptide 4 differed from peptides 3 and 5 with the PPII/PPI populations strongly predominating in both water and chloroform. Thus, the (2*S*)- CF_3 C^δ -substitution of pseudoproline appears valuable for stabilizing the ϕ and ψ torsion angles into PP-like structures in apolar environments.

Effects of (2)- CF_3 Substitution on Puckering. Comparison of the puckering parameters of the optimized local minima of peptides 3–5 allowed us to explore the effects of the (2)- CF_3 substitution on the puckering of pseudoproline Oxa. The parameters χ_m and P ,⁴⁸ which correspond to the puckering amplitude and the phase angle, respectively, are listed in Tables S1 and S2 and averaged in Table S3 of the Supporting Information. Both the down- and up-puckered structures of the unsubstituted peptide 3 had almost the same puckering

amplitude of 39° and the phase angles of 178° and 18°, respectively, whatever the peptide bond geometry or the solvent polarity. Each of the down puckering of the (2*S*)- CF_3 peptide 4 and the up puckering of the (2*R*)- CF_3 peptide 5 had almost the same amplitude and phase angle, irrespective of the prolyl peptide bond and the solvent polarity, but their amplitudes were decreased by ~10° compared to peptide 3. On the contrary, the puckerings of the up structures of peptide 4 and the down structures of peptide 5 are strongly influenced by the prolyl peptide bond and/or solvent polarity. Compared with peptide 3, the largest changes in puckering are found for the *trans*-up structures of peptide 4 and the *trans*-down structures of peptide 5, whereas the *cis*-down structures of peptide 5 had almost the same puckering amplitudes and phase angles as those of peptide 3 in chloroform and water.

A detailed analysis of the pseudoproline's geometries indicated that there is no direct correlation between the ring puckerings and the ability for the backbone to adopt a γ -turn conformation. In particular, it is found that different puckerings are compatible with a H-bond for the *trans* conformers, peptides 3 and 5 being characterized by a down ($\chi_m = 38^\circ$, $P = 179^\circ$) and an up ($\chi_m = 29^\circ$, $P = 20^\circ$) puckering, respectively. Moreover, for these two peptides, changing chloroform to water was accompanied by the disruption of H-bond, but by only very subtle effects on the puckering parameters. Importantly, the minimized structures revealed the origin of the puckering stabilities. They showed evidence of favored electrostatic interactions between the negatively charged F atoms (−0.35 e) of the CF_3 group and positively charged atoms in close contact, in particular the H atoms of the $C^\beta H_2$ group (+0.21 e). As an example, we display in Figure 4a the minimized structures of peptide 4 in water, where the $d(F\cdots H-C^\beta) = 2.50$ Å and the $d(F\cdots H-C_{Ac}) = 2.45$ Å of the privileged *tFd* conformation are shorter by ~1.1 and ~0.3 Å than those of conformation *tFu*, respectively. Inverse

observations are made for peptide **5**, explaining the higher stability of the up puckerings for this peptide (see section S2 of the Supporting Information). Moreover, overlaps of the C^{δ} -F antibonding orbitals (σ^*) with all bonding (σ) and lone pair (LP) orbitals have been analyzed in order to understand the puckering preferences (section S3 of the Supporting Information). Although energies due to hyperconjugation were found weaker than for electrostatic interactions, it appeared that $\sigma(C^{\delta}-H) \rightarrow \sigma^*(C^{\delta}-F)$ and $LP(O') \rightarrow \sigma^*(C^{\delta}-F)$ interactions also contribute to the stabilization of the down puckering (respectively, up puckering) of the peptide **4** (respectively, peptide **5**). Figure 4b illustrates the orbital overlaps for peptide **4** in water. On the *tFd* conformer, calculations gave 3.57 and 1.44 kcal/mol for the down puckering for the $\sigma(C^{\delta}-H) \rightarrow \sigma^*(C^{\delta}-F)$ and $LP(O') \rightarrow \sigma^*(C^{\delta}-F)$ interactions, respectively, which were higher by 0.19 and 0.25 kcal/mol, respectively, compared with the energies calculated for the *tFu* conformer (see Table S6 of the Supporting Information).

Thermodynamic Characteristics of the *Cis-Trans* Isomerization. The structural properties of the ground states and the transition states of the two diastereomers were also analyzed to understand how the (2*S*)-CF₃ substitution could impact the *cis-trans* isomerization rate. Previously, both changes in charge of the prolyl nitrogen and decrease in electron overlap of the C-N bond for the transition state were suggested to play a role in lowering the rotational barrier of the unsubstituted peptide **3** compared to the Pro peptide.¹⁷ In order to unveil the changes associated with the (2)-CF₃ substitution, the bond length, bond index, and the charges of the carbonyl C and the prolyl nitrogen of the C-N bond have been compared for the privileged *trans* and *ts* conformers for peptides **3-5** (Table S7 of the Supporting Information). Unfortunately, this approach failed to explain the lower rotational barrier ΔG^{\ddagger}_{tc} observed for peptide **5**, since (i) almost identical bond lengths were found for peptide **4** and **5** and (ii) similar charge separation during the isomerization process were calculated for peptide **3** and **5** (section S4 of the Supporting Information). Besides, no intramolecular H-bond between the cyclic nitrogen and the following amide proton could be localized in the transition state of the (2*R*)-CF₃ peptide **5** (section S5 of the Supporting Information), although such intramolecular H-bond was capable of efficiently catalyzing the prolyl isomerization in some model peptides.⁴⁹

The electronic single-point energies ($E_{e,sp}$) and solvation free energies (ΔG_s) of the privileged *trans*, *cis*, and *ts* structures for peptides **4** and **5** in chloroform and water were compared to each other, in order to determine the origin of the lower values of the rotational barriers ΔG^{\ddagger}_{tc} and ΔG^{\ddagger}_{ct} for the *trans-cis* isomerization of peptide **5** compared to those of peptide **4**, as found by NMR and theoretical calculations. As described in section S6 of the Supporting Information, significantly lower values (~ 7 kcal/mol) were calculated for the electronic single-point energies $E_{e,sp}$ of the transition states of peptide **5** compared to those of peptide **4** in both chloroform and water. On the other hand, $E_{e,sp}$ and ΔG_s of the ground states were very similar for the two peptides in water, whereas the moderate variations of $E_{e,sp}$ offset the ΔG_s in chloroform and led to comparable values of $E_c = E_{e,sp} + \Delta G_s$. Thus, the lower ΔE^{\ddagger}_{tc} and ΔE^{\ddagger}_{ct} barriers of peptide **5** were a direct consequence of the lower $E_{e,sp}$ of *ts1* for (2*R*)-CF₃ peptide **5** than that of *ts2* for (2*S*)-CF₃ peptide **4**. As done for puckering preference, the close contacts of the F atoms of the CF₃ group with neighboring

atoms were monitored for their transition states. It was found that *ts1* of (2*R*)-CF₃ peptide **5** had the favored electrostatic interactions between the negatively charged F atom (-0.35 e) and the positively charged amide H atom ($+0.40$ e) of the C-terminal group with $d(F \cdots H-N) = 2.64$ Å in chloroform and 2.72 Å in water. This close contact appeared as a characteristic feature of the transition states of peptide **5** since it did not exist for any local minima identified for both (2*S*)-CF₃ peptide **4** and (2*R*)-CF₃ peptide **5** in chloroform and water. For peptide **4**, *ts2* had the unfavorable electrostatic contact between the positively charged H $^{\alpha}$ atom ($+0.18$ e) and the positively charged amide H atom ($+0.40$ e) with $d(H^{\alpha} \cdots H-N) = 2.69$ Å in chloroform and 2.66 Å in water.

Finally, the second-order perturbation energies of the $\sigma^*(C^{\delta}-F)$ antibonding orbitals with all bonding and LP orbitals of *ts2* and *ts1* for (2*S*)- and (2*R*)-diastereomers **4** and **5**, respectively, were analyzed in order to understand their contribution to their relative stabilities.^{43b} The total second-order perturbation energies of these two transition states are listed in Table S8 of the Supporting Information, to which the important terms are listed in Table S9 of the Supporting Information. The total second-order perturbation energies of *ts1* for (2*R*)-diastereomer **5** were slightly larger than those of *ts2* for (2*S*)-diastereomer **4** by 0.71 and 0.99 kcal/mol in chloroform and water, respectively, to which the $LP \rightarrow \sigma^*(C^{\delta}-F)$ interactions contribute dominantly. Indeed, although the $\sigma(C^{\delta}-H) \rightarrow \sigma^*(C^{\delta}-F_a)$ hyperconjugations were associated with the largest energies for both peptides (~ 3.88 kcal/mol), the $LP(N) \rightarrow \sigma^*(C^{\delta}-F_-)$ and $LP(O') \rightarrow \sigma^*(C^{\delta}-F_+)$ interactions differed the most from peptide **4** to **5** (ca. $+0.55$ kcal/mol), which contributed in lowering the $E_{e,sp}$ of *ts1* for peptide **5**.

Unique Properties of the C^{δ} -Substituted CF₃-Pseudo-prolines. Numerous proline analogues have been described previously, including C^{α} -, C^{β} -, C^{γ} -, and C^{δ} -substituted pyrrolidine rings, which signify the great interest for these building blocks to design conformationally restrained peptides.⁵⁰⁻⁶² In particular, C^{γ} -substituted proline residues have been developed as analogues of the C^{γ} -(*R*)-hydroxyproline (Hyp), in order to be inserted in the collagen protein. Hyp is a major component of collagen, playing a key role for its stability. Thus, small electron-withdrawing substituents as F,⁵⁰ Cl,⁵⁴ NH₂,⁵⁵ or N₃⁵⁶ have been assessed for their ability to reinforce the collagen PPII helix. It was shown that their inductive effects was responsible for energetic changes of the prolyl peptide bond, decreasing the pK_a of the prolyl nitrogen, lowering the C-N bond order, and thus facilitating the *cis-trans* isomerization of the peptide bond.⁵⁰ These inductive effects were thought to enhance the stability of collagen via an acceleration of the folding process. Similarly, the presence of the oxygen atom in the oxazolidine ring **3** induces an electron-withdrawing effect. The atomic charge of the prolyl nitrogen for the oxazolidine peptide **3** becomes more negative by ~ 0.1 e than that of the Pro peptide.¹⁷ Incorporating the strongly electro-negative CF₃ at the C^{δ} position was expected to further enhance electronic effects. Herein, we have shown that the electronic effect induced by the CF₃ group results in lengthening of the C^{δ} -N bond and decreasing of the bond overlap for both C^{δ} -(*R*)/(*S*)-CF₃ oxazolidine peptides in solution. In addition, the C^{δ} -CF₃ substitution led to more positive δ_C and negative δ_N atomic charges, which indicates that the C-N bond of both C^{δ} -(*R*)/(*S*)-CF₃ oxazolidine peptides becomes more ionic for the *trans* and *ts* conformers. A major

property that distinguishes the two C^δ-substituted oxazolidines from each other is the marked difference of the electronic energy of their respective transition states. According to our quantum-mechanical results, electronic energy of ts1 in peptide 5 is lower by ~6 kcal/mol than the one of ts2 in peptide 4. This probably explains the weaker energy barrier found for the C^δ-(R)-CF₃ oxazolidine peptide compared with the C^δ-(S)-CF₃ oxazolidine peptide. Referring to the proline peptide, the decrease of the *cis*–*trans* isomerization barrier is then ~4 kcal/mol, corresponding to ~20% of the prolyl barrier. Beyond the interest of this amino acid residue for the design of collagen analogues, for example, such an enhancement of the *cis*/*trans* interconversion rate may be very valuable for the biological processes that rely on this molecular switch.⁶³

The works of Raines et al., later confirmed by others groups, have also demonstrated that the pucker of a pyrrolidine ring can be influenced by the electronegative C^γ-substituents through hyperconjugative delocalization.^{57–60} The driving force of the observed *gauche* effect would be due to hyperconjugative donation from the $\sigma(\text{C}^\beta\text{--H})_{\text{ax}}$ and $\sigma(\text{C}^\delta\text{--H})_{\text{ax}}$ bonding orbitals into the $\sigma^*(\text{C}^\gamma\text{--X})$ antibonding orbital, where X is the electronegative atom. Thus, the electron-withdrawing hydroxyl group in C^γ(R)-hydroxyproline was found to strongly stabilize the up puckering, whereas the C^γ(S)-hydroxyproline was associated with a down puckering. Although such strong $\sigma \rightarrow \sigma^*$ hyperconjugations do not occur in pseudoproline, the favored lone pair of O^γ to $\sigma^*(\text{C}^\epsilon\text{--F})$ interactions by ~1 kcal/mol appear to contribute in stabilizing the preferred down and up puckerings of (2S)- and (2R)-CF₃-Oxa pseudoproline, respectively. Importantly, it is herein demonstrated that ring puckerings can be strongly constrained by the C^δ substituent, the (2R)-Ψ^{CF₃,H}Pro being up-puckered and the (2S)-Ψ^{H,CF₃}Pro being down-puckered, which can be ascribed to the favored electrostatic interactions between the F atom of the CF₃ group and the H atom of the C^βH₂ group. Interestingly, both compounds share the same PPII backbone conformation, whereas analysis of X-ray structures of natural peptides and proteins have shown that prolyl puckerings generate singular backbone conformation.^{2,8,9}

Finally, C^δ-alkyl substituents have been described for their ability to stabilize the *cis* conformation of the preceding proline peptide bond. Delaney and Madison carried out NMR experiments on the C^δ-methylated Pro peptides, which showed that the steric interactions of the 5-methyl group destabilize the *trans* conformer for the (5S)-Me-Pro peptide without affecting the prolyl isomerization barrier, whereas *cis* and *trans* conformers for the (5R)-Me-Pro peptide are destabilized by the same amount so that the barrier is lowered without altering the equilibrium.¹¹ Lubell et al. showed that steric interactions imposed by the bulky 5-*tert*-butyl were responsible for the control the peptide bond geometry.^{12,45,64} The (5S)- and (5R)-*t*-Bu substitutions increased the *cis* peptide bond up to 70% and 50% compared to the Pro peptide in water. However, only the (5R)-*t*-Bu substitution decreased the rotational barrier by ~4 kcal/mol, which is similar to that of pseudoproline in water. This decrease was attributed to the fact that the bulky substituent in C^δ-position skews away the amide bond from planarity. Mutter et al. have demonstrated the similar effects on 5-substituted pseudoproline.^{13–15} The substitution by (2S)-*p*-methoxyphenyl (PMP) generally led to higher *cis* contents for ΨPro-containing tetrapeptides by ~30% than the (2R)-PMP substitution but the former diastereomer led to the higher prolyl rotational barriers by ~2 kcal/mol.¹⁴ Finally, Jamet et al.

reported that the (2S)-methyl substitution brought the higher *cis* population of 75% for the thiazolidine peptide in chloroform, whereas the (2R)-methyl substitution did not enhance the *cis* content. Therefore, these previous studies indicate that the (S)-substitution on C^δ-position enhanced the *cis* content and prolyl rotational barrier for Pro- and ΨPro-containing peptides over the (R)-substitution, although the *cis* population and prolyl rotational barrier are likely to depend on the substituent, the length of peptide, and the solvent polarity. Herein, we established that the combination of the steric and electronic effects of the (2R)-Ψ^{CF₃,H}Pro makes it possible to greatly reduce the *cis*–*trans* isomerization barrier with only moderate consequences on the *cis*/*trans* population. In particular, the favored electrostatic interactions between the F atom of the CF₃ group and the amide H atom of the C-terminal group and the hyperconjugations of the lone pair of O^γ to $\sigma^*(\text{C}^\epsilon\text{--F})$ appear to contribute in lowering the rotational barriers of (2R)-CF₃-Oxa residue.

CONCLUSIONS

As described previously, the presence of the ring oxygen in the proline-like oxazolidines is accompanied with an enhanced proline effect. Compared with Xaa-Pro moieties, greater *cis*/*trans* population ratio and enhanced isomerization rates were reported for the Xaa–ΨPro peptide bonds (Xaa = Ala, Val). Although such a global behavior is observed for peptides 3–5, it is herein shown that a separate control of the two effects is possible, which relies on the configuration of the CF₃ substituent. In all the solvents tested, the (2R)-CF₃ substitution (peptide 5) was associated with ca. 2 kcal/mol decreases of the rotational barriers, whereas the (2S)-CF₃ substitution had virtually no effect on the isomerization rates. Besides, in chloroform and DMSO, only the (2S)-CF₃ substitution (peptide 4) was able to markedly enhance the *cis* population. Theoretical calculations gave some insights into the electronic and geometric effects of the CF₃ group, allowing a unified view between the NMR observations and the quantum-mechanical results. In all cases, the presence of the CF₃ group dramatically reduces the dynamic of the oxazolidine ring but also acts on the backbone torsion angles ϕ and ψ . Interestingly, PPII/PPI torsion angles are greatly favored in water, whereas PP_{II}/PP_I-like or γ -turn conformations predominate in chloroform for (2)-CF₃ substituted peptides 4 or 5, respectively. Thus, CF₃ group appears to be very valuable for locally tuning the peptide conformation and for promoting the *cis*–*trans* isomerization process.

ASSOCIATED CONTENT

Supporting Information

Complete ref 33. NMR Spectra of peptides 3–5 in CDCl₃, DMSO, and water. Synthesis of peptide 3. Geometrical features, thermodynamic properties, and electronic population analysis of local minima and transition states for peptides 3–5 calculated at the B3LYP/6-311++G(d,p)//CPCM HF/6-31+G(d) level of theory in chloroform and water. This material is available free of charge via the Internet at <http://pubs.acs.org>.

AUTHOR INFORMATION

Corresponding Author

*E-mail: emerich.miclet@upmc.fr (E.M.); ykkang@chungbuk.ac.kr (Y.K.K.). Fax: +33 1 44 27 38 43 (E.M.); +82 43 273 8328 (Y.K.K.).

Notes

The authors declare no competing financial interest.

ACKNOWLEDGMENTS

D.F. is a postdoctoral researcher of the Fund for Scientific Research Flanders (FWO-Vlaanderen). The authors are grateful to Véronique Doan for her contribution to the preparation of analogue 3 and David L. Bryce for stimulating discussions. T.B. thanks Central Glass Co. for financial support. Y.K.K. thanks the National Research Foundation of Korea (NRF) for support (No. 2011-0025717).

REFERENCES

- Momany, F. A.; McGuire, R. F.; Burgess, A. W.; Scheraga, H. A. *J. Phys. Chem.* **1975**, *79*, 2361–2381.
- Pal, D.; Chakrabarti, P. *J. Mol. Biol.* **1999**, *294*, 271–288.
- Stewart, D. E.; Sarkar, A.; Wampler, J. E. *J. Mol. Biol.* **1990**, *214*, 253–260.
- Jabs, A.; Weiss, M. S.; Hilgenfeld, R. *J. Mol. Biol.* **1999**, *286*, 291–304.
- Balasubramanian, R.; Lakshminarayanan, A. V.; Sabesan, M. N.; Tegoni, G.; Venkatesan, K.; Ramachandran, G. N. *Int. J. Protein Res.* **1971**, *3*, 25–33.
- DeTar, D. F.; Luthra, N. P. *J. Am. Chem. Soc.* **1977**, *99*, 1232–1244.
- Madison, V. *Biopolymers* **1977**, *16*, 2671–2692.
- Milner-White, E. J.; Bell, L. H.; Maccallum, P. H. *J. Mol. Biol.* **1992**, *228*, 725–734.
- Vitagliano, L.; Berisio, R.; Mastrangelo, A.; Mazzarella, L.; Zagari, A. *Protein Sci.* **2001**, *10*, 2627–2632.
- Dugave, C.; Demange, L. *Chem. Rev.* **2003**, *103*, 2475–2532.
- Delaney, N. G.; Madison, V. *Int. J. Pept. Protein Res.* **1982**, *19*, 543–548.
- Beausoleil, E.; Lubell, W. D. *J. Am. Chem. Soc.* **1996**, *118*, 12902–12908.
- Dumy, P.; Keller, M.; Ryan, D. E.; Rohwedder, B.; Wöhr, T.; Mutter, M. *J. Am. Chem. Soc.* **1997**, *119*, 918–925.
- Keller, M.; Sager, C.; Dumy, P.; Schutkowski, M.; Fischer, G. S.; Mutter, M. *J. Am. Chem. Soc.* **1998**, *120*, 2714–2720.
- Jamet, H.; Jourdan, M.; Dumy, P. *J. Phys. Chem. B* **2008**, *112*, 9975–9981.
- Kang, Y. K. *THEOCHEM* **2002**, *585*, 209–221.
- Kang, Y. K. *J. Phys. Chem. B* **2002**, *106*, 2074–2082.
- Kang, Y. K.; Choi, H. Y. *Biophys. Chem.* **2004**, *111*, 135–142.
- Kang, Y. K. *J. Phys. Chem. B* **2006**, *110*, 21338–21348.
- Kang, Y. K. *J. Phys. Chem. B* **2007**, *111*, 10550–10556.
- Kang, Y. K.; Park, H. S. *J. Phys. Chem. B* **2007**, *111*, 12551–12562.
- Kang, Y. K.; Park, H. S.; Byun, B. J. *Biopolymers* **2009**, *91*, 444–455.
- (a) Huguenot, F.; Brigaud, T. *J. Org. Chem.* **2006**, *71*, 7075–7078. (b) Chaume, G.; Van Severen, M.-C.; Marinkovic, S.; Brigaud, T. *Org. Lett.* **2006**, *8*, 6123–6126. (c) Chaume, G.; Van Severen, M.-C.; Ricard, L.; Brigaud, T. *J. Fluorine Chem.* **2008**, *129*, 1104–1109. (d) Caupène, C.; Chaume, G.; Ricard, L.; Brigaud, T. *Org. Lett.* **2009**, *11*, 209–212. (e) Simon, J.; Nguyen, T. T.; Chelain, E.; Lensen, N.; Pytkowicz, J.; Chaume, G.; Brigaud, T. *Tetrahedron: Asymmetry* **2011**, *22*, 309–314. (f) Chaume, G.; Lensen, N.; Caupène, C.; Brigaud, T. *Eur. J. Org. Chem.* **2009**, 5717–5724.
- Chaume, G.; Barbeau, O.; Lesot, P.; Brigaud, T. *J. Org. Chem.* **2010**, *75*, 4135–4145.
- The size of a trifluoromethyl group is evaluated to be close to an isopropyl group. Leroux, F. *ChemBioChem* **2004**, *5*, 644–649.
- O'Hagan, D. *Chem. Soc. Rev.* **2008**, *37*, 308–319.
- (a) Uneyama, K. In *Fluorine in Medicinal Chemistry and Chemical Biology*; Ojima, I., Ed.; John Wiley & Sons Ltd.: Chichester, UK, 2009; pp 213–256. (b) Zanda, M. *New J. Chem.* **2004**, *28*, 1401–1411 and references cited therein. (c) Molteni, M.; Pesenti, C.; Sani, M.; Volonterio, A.; Zanda, M. *J. Fluorine Chem.* **2004**, *125*, 1735–1743 and references cited therein. (d) Barth, D.; Milbradt, A. G.; Renner, C.; Moroder, L. *ChemBioChem* **2004**, *5*, 79–86. (e) Smits, R.; Cadicamo, C. D.; Burger, K.; Kokschi, B. *Chem. Soc. Rev.* **2008**, *37*, 1727–1739 and references therein. (f) Qiu, X.-L.; Qing, F.-L. *Eur. J. Org. Chem.* **2011**, *18*, 3261–3278.
- (a) Jaekel, C.; Kokschi, B. *Eur. J. Org. Chem.* **2005**, 4483–4503. (b) Yoder, N. C.; Kumar, K. *Chem. Soc. Rev.* **2002**, *31*, 335–341. (c) Meng, H.; Kumar, K. *J. Am. Chem. Soc.* **2007**, *129*, 15615–15622. (d) Kokschi, B.; Sewald, N.; Hofmann, H.-J.; Burger, K.; Jakubke, H.-D. *J. Pept. Sci.* **1997**, *3*, 157–167.
- (a) Miclet, E.; Boissbouvier, J.; Bax, A. *J. Biomol. NMR* **2005**, *31*, 201–216. (b) Miclet, E.; Williams, D. C.; Clore, G. M.; Bryce, D. L.; Boissbouvier, J.; Bax, A. *J. Am. Chem. Soc.* **2004**, *126*, 10560–10570.
- Guichard, G.; Violette, A.; Chassaing, G.; Miclet, E. *Magn. Reson. Chem.* **2008**, *46*, 918–924.
- Williams, D. H.; Fleming, I. *Spectroscopic Methods in Organic Chemistry*, 4th ed.; McGraw-Hill: London, 1987.
- Friebolin, H. *Basic One- and Two-dimensional NMR Spectroscopy*; VCH Verlagsgesellschaft: Weinheim, Germany, 1991.
- Frisch, M. J.; Trucks, G. W.; Schlegel, H. B.; Scuseria, G. E.; Robb, M. A.; Cheeseman, J. R.; Montgomery, J. A., Jr.; Vreven, T.; Kudin, K. N.; Burant, J. C. et al. *Gaussian 03, revision D.01*; Gaussian, Inc.: Wallingford, CT, 2004.
- Frisch, A.; Dennington, R. D., II; Keith, T. A. *GaussView, version 3.0*; Gaussian, Inc.: Carnegie, PA, 2003.
- (a) Barone, V.; Cossi, M. *J. Phys. Chem. A* **1998**, *102*, 1995–2001. (b) Cossi, M.; Rega, N.; Scalmani, G.; Barone, V. *J. Comput. Chem.* **2003**, *24*, 669–681.
- (a) Barone, V.; Cossi, M.; Tomasi, J. *J. Chem. Phys.* **1997**, *107*, 3210–3221. (b) Cossi, M.; Scalmani, G.; Rega, N.; Barone, V. *J. Chem. Phys.* **2002**, *117*, 43–54.
- Fischer, S.; Dunbrack, R. L., Jr.; Karplus, M. *J. Am. Chem. Soc.* **1994**, *116*, 11931–11937.
- (a) Gonzalez, C.; Schlegel, H. B. *J. Chem. Phys.* **1989**, *90*, 2154–2161. (b) Gonzalez, C.; Schlegel, H. B. *J. Phys. Chem.* **1990**, *94*, 5523–5527.
- Foresman, J. B.; Frisch, A. *Exploring Chemistry with Electronic Structure Methods*, 2nd ed.; Gaussian, Inc.: Pittsburgh, PA, 1996; Chapter 8.
- Kang, Y. K. *THEOCHEM* **2001**, *546*, 183–193.
- Hehre, W. J.; Radom, L.; Schleyer, P. v. R.; Pople, J. A. *Ab Initio Molecular Orbital Theory*; John Wiley & Sons: New York, 1986; Chapter 6.
- Frisch, A.; Frisch, M. J.; Trucks, G. W. *Gaussian 03 User's Reference, version 7.0*; Gaussian, Inc.: Pittsburgh, PA, 2003.
- (a) Brunck, T. K.; Weinhold, F. *J. Am. Chem. Soc.* **1979**, *101*, 1700–1709. (b) Weinhold, F. In *Encyclopedia of Computational Chemistry*; Schleyer, P. v. R., Allinger, N. L., Clark, T., Gasteiger, J., Kollman, P. A., Schaefer, H. F., III, Schreiner, P. R., Eds.; Wiley: Chichester, UK, 1998; Vol. 3, p 1792.
- Wiberg, K. B. *Tetrahedron* **1968**, *24*, 1083–1096.
- Halab, L.; Lubell, W. D. *J. Org. Chem.* **1999**, *64*, 3312–3321.
- Kessler, H. *Angew. Chem., Int. Ed.* **1982**, *21*, 512–523.
- Stein, R. L. *Adv. Protein Chem.* **1993**, *44*, 1–24 and references therein.
- Altona, C.; Sundaralingam, M. *J. Am. Chem. Soc.* **1972**, *94*, 8205–8212.
- Cox, C.; Lectka, T. *J. Am. Chem. Soc.* **1998**, *120*, 10660–10668.
- Eberhardt, E. S.; Panasik, N., Jr.; Raines, R. T. *J. Am. Chem. Soc.* **1996**, *118*, 12261–12266.
- Calaza, M. I.; Cativiela, C. *Eur. J. Org. Chem.* **2008**, 3427–3448.
- Quancard, J.; Labonne, A.; Jacquot, Y.; Chassaing, G.; Lavielle, S.; Karoyan, P. *J. Org. Chem.* **2004**, *69*, 7940–7948.
- Jacquot, Y.; Broutin, I.; Miclet, E.; Nicaise, M.; Lequin, O.; Goasdoué, N.; Joss, C.; Karoyan, P.; Desmadril, M.; Ducruix, A.; Lavielle, S. *Bioorg. Med. Chem.* **2007**, *15*, 1439–1447.
- Shoulders, M. D.; Raines, R. T. *Adv. Exp. Med. Biol.* **2009**, *611*, 251–252.

- (55) Babu, I. R.; Ganesh, K. N. *J. Am. Chem. Soc.* **2001**, *123*, 2079–2080.
- (56) Sonntag, L.-S.; Schweizer, S.; Ochsenfeld, C.; Wennemers, H. *J. Am. Chem. Soc.* **2006**, *128*, 14697–14703.
- (57) Holmgren, S. K.; Taylor, K. M.; Bretscher, L. E.; Raines, R. T. *Nature* **1998**, *392*, 666–667.
- (58) Weinhold, F. *Nature* **2001**, *411*, 539–541.
- (59) Bretscher, L. E.; Jenkins, C. L.; Taylor, K. M.; DeRider, M. L.; Raines, R. T. *J. Am. Chem. Soc.* **2001**, *123*, 777–778.
- (60) Shoulders, M. D.; Hodges, J. A.; Raines, R. T. *J. Am. Chem. Soc.* **2006**, *128*, 8112–8113.
- (61) Kang, Y. K.; Byun, B. J.; Park, H. S. *Biopolymers* **2011**, *95*, 51–61.
- (62) Taylor, C. M.; Hardré, R.; Edwards, P. J. B. *J. Org. Chem.* **2005**, *70*, 1306–1315.
- (63) Andreotti, A. H. *Biochemistry* **2003**, *42*, 9515–9524.
- (64) Halab, L.; Lubell, W. D. *J. Am. Chem. Soc.* **2002**, *124*, 2474–2484.